JCB Article

Dynamics of ligand-induced, Rac1-dependent anchoring of cadherins to the actin cytoskeleton

Mireille Lambert,[1] Daniel Choquet,[2] and René-Marc Mège[1]

[1]Signalisation et Différenciation Cellulaires dans les Systèmes Nerveux et Musculaire, INSERM U440, Université Paris 6, Institut du Fer à Moulin, 75005 Paris, France
[2]Physiologie Cellulaire de la Synapse, UMR CNRS 5091-Université Bordeaux 2, Institut François Magendie, 33077 Bordeaux cedex, France

Cadherin receptors are key morphoregulatory molecules during development. To dissect their mode of action, we developed an approach based on the use of myogenic C2 cells and beads coated with an Ncad-Fc ligand, allowing us to mimic cadherin-mediated adhesion. We used optical tweezers and video microscopy to investigate the dynamics of N-cadherin anchoring within the very first seconds of bead–cell contact. The analysis of the bead movement by single-particle tracking indicated that N-cadherin molecules were freely diffusive in the first few seconds after bead binding. The beads rapidly became diffusion-restricted and underwent an oriented rearward movement as a result of N-cadherin anchoring to the actin cytoskeleton. The kinetics of anchoring were dependent on ligand density, suggesting that it was an inducible process triggered by active cadherin recruitment. This anchoring was inhibited by the dominant negative form of Rac1, but not that of Cdc42. The Rac1 mutant had no effect on cell contact formation or cadherin–catenin complex recruitment, but did inhibit actin recruitment. Our results suggest that cadherin anchoring to the actin cytoskeleton is an adhesion-triggered, Rac1-regulated process enabling the transduction of mechanical forces across the cell membrane; they uncover novel aspects of the action of cadherins in cell sorting, cell migration, and growth cone navigation.

Introduction

The highly conserved cell adhesion molecules of the cadherin family constitute one of the major classes of receptors mediating juxtacrine cell interactions. Cadherins are key morphoregulatory molecules involved in developmental processes (Takeichi, 1988; Yap et al., 1997). Their contribution to cell aggregation and segregation is essential for embryogenesis and histogenesis (Friedlander et al., 1989). N-cadherin is involved in the organization and functional regulation of various tissues, including the nervous system and cardiac and skeletal muscles (Hatta et al., 1988; Radice et al., 1997). In the nervous system, N-cadherin is expressed in a combinatorial fashion with other members of the cadherin family throughout development, and is thought to participate in neuronal cell sorting and neurite outgrowth, as well as synapse formation, maturation, and plasticity (Benson et al., 2001). N-cadherin has also been implicated in myogenic precursor cell migration (Brand-Saberi et al., 1996) and differentiation (Goichberg and Geiger, 1998), as well as in myoblast fusion (Mège et al., 1992).

Cadherins are transmembrane glycoproteins that mediate cell–cell adhesion through homophilic Ca^{2+}-dependent interactions of their extracellular region and anchoring of their intracellular domain to the actin cytoskeleton (Yap et al., 1997). Cadherin ectodomains are thought to dimerize and to interact with dimers of the same cadherin species at the surface of adjacent cells (Shapiro et al., 1995; Pertz et al., 1999). On the other hand, the conserved cytoplasmic domain of cadherins is part of a multimolecular complex including the p120 phosphoprotein and catenins α and β, which link cadherins to the actin cytoskeleton and have a modulatory effect on cadherin adhesive function (Kemler, 1993; Anastasiadis and Reynolds, 2000). The integrity of this cadherin–catenin complex and its correct association to the actin cytoskeleton are required for cell aggregation (Nagafuchi and Takeichi, 1988).

Although the developmental roles of cadherins are well documented, their mode of action is still a matter of intense investigation. In addition to the increasing understanding of the molecular mechanisms underlying specific adhesive interactions, other aspects (i.e., the dynamics and mechanisms

Address correspondence to René-Marc Mège, INSERM U440, 17 rue du Fer à Moulin, 75005 Paris, France. Tel.: 33-1-45-87-61-36. Fax: 33-1-45-87-61-32. E-mail: mege@ifm.inserm.fr

Key words: cell adhesion; cytoskeleton; signal transduction; migration; mechanotransduction

of cell contact formation and the nature of the mechanochemical signals transduced in response to contact formation) remain largely unknown. Recently, we developed an approach allowing us to mimic and control cadherin function in the absence of actual cell–cell contact (Lambert et al., 2000). We produced a fusion protein containing the N-cadherin ectodomain fused to the IgG Fc fragment (Ncad-Fc), which retains the homophilic Ca^{2+}-dependent adhesive properties of native N-cadherin. Ncad-Fc–coated beads specifically bind to N-cadherin–expressing cells, fully mimicking the formation of cell–cell contacts. The bead binding induces the recruitment of preexisting cell membrane cadherin–catenin complexes, and triggers the recruitment of tyrosine-phosphorylated proteins and the redistribution of actin filaments. These results support a model in which the homophilic adhesion of cadherin ectodomains induces the transduction of mechanochemical signals toward the intracellular signaling apparatus and the actin cytoskeleton. The signaling toward actin filaments might be of major importance, not only for the strengthening of cell–cell contacts (Adams and Nelson, 1998; Vasioukhin et al., 2000), but also for the coupling of cadherin-based adhesion to the force-generating moving actin cytoskeleton. Although this question has been extensively studied for extracellular matrix adhesion receptors of the integrin family (Miyamoto et al., 1995a; Lauffenburger and Horwitz, 1996; Choquet et al., 1997), little is known in the case of cadherins.

Because of its importance in providing the driving force for cell sorting, cell migration, and growth cone navigation, we focused on the dynamics of functional anchoring of cadherins to the actin cytoskeleton, thus allowing the transduction of mechanical forces across the cell membrane. We combined our cellular model with a biophysical approach, enabling us to monitor the bidimensional movement of single or small clusters of proteins and to determine their level of anchoring to the cytoskeleton (Kusumi et al., 1993; Simson et al., 1995). Indeed, the movement of ligand-coated microparticles bound to membrane receptors can be monitored with nanometer precision by video microscopy and single-particle tracking (Sterba and Sheetz, 1998). So far it has been possible to follow (Kusumi et al., 1999) the anchoring of integrins or E-cadherin to the cytoskeleton (Choquet et al., 1997; Sako et al., 1998; Felsenfeld et al., 1999; Nishizaka et al., 2000). In the present work, N-cadherin molecules were triggered at the surface of C2 myogenic cells with Ncad-Fc–coated beads. Optical tweezers were used to force the contact of the beads with different domains of the cell membrane. The dynamics of N-cadherin anchoring to the cytoskeleton were analyzed in the very first seconds after bead–cell contact. We observed that N-cadherin receptors were initially free to undergo Brownian diffusion, and then became tightly anchored to the actin cytoskeleton. Ligand dose effect analysis, pharmacological perturbations, and cell transfection were used to approach the molecular mechanisms controlling this anchoring. Altogether, our results show for the first time the dynamics and molecular mechanisms leading to the anchoring of cadherins to the actin cytoskeleton, uncovering novel aspects of the mode of action of these adhesion receptors.

Results

Ncad-Fc beads specifically bind to the tip of C2 cell lamellipodia and display an actin-dependent rearward transport

To tightly control N-cadherin engagement in time and space, 1-μm latex beads coated with the highly active Ncad-Fc ligand were trapped in a laser beam and held for a few seconds on the free cell surface to force bead–cell contact (Fig. 1 A). Ncad-Fc beads were applied on the lamellipodia of motile myogenic C2 cells expressing endogenous N-cadherin. In most cases, forcing the bead–cell contact for only 5 s resulted in a stable attachment of Ncad-Fc beads at the surface of the cell (85%, $n = 219$). In contrast, only 1/4 of the control Fc-coated beads remained bound at the cell surface after the laser beam was turned off (Table I). Thus, Ncad-Fc–coated beads established a specific N-cadherin–mediated adhesion with the surface of C2 cells. This adhesion was dependent on the presence of extracellular Ca^{2+} as shown by the reduced attachment of beads to the cell in the presence of EGTA. This binding was stable, as no bead release was observed during the 50–200 s after the forced interaction. Moreover, we observed that forcing the Ncad-Fc bead to contact the cell body did not lead to stable binding, indicating that the N-cadherin–mediated bead binding was only efficient on the lamellipodia. Thus, all subsequent experiments were performed by applying beads on this domain of the cell membrane.

To gain information about the mobility of N-cadherin, video images were recorded over 50– 200 s, and bead trajectories were analyzed by single-particle tracking (Fig. 1, B and C). Most of the Ncad-Fc beads instantaneously adopted a directed movement toward the rear of the lamellipodia, and their apparent two-dimensional diffusion co-

Table I. **Binding capability of Ncad-Fc–coated beads**

Bead coverage	Attached beads	Number of tested beads	Percentage binding
High Ncad-Fc	185	219	84
Medium Ncad-Fc	56	72	78
Low Ncad-Fc	25	39	64
High Ncad-Fc + EGTA	15	32	47
Fc	19	72	26

1-μm latex beads were loaded at maximal charge (High), or with decreasing densities of Ncad-Fc corresponding to 30 % (Medium) and 10 % (Low) of the maximal charge. Bead binding was assessed on the lamellipodia of motile myogenic C2 cells as described in Fig. 1. Ncad-Fc conferred specific binding properties to coated beads, significative over background binding of Fc-coated beads (Fc) ($P < 0.0001$, C2 test). This binding efficiency of Ncad-Fc beads was highly reduced in the presence of 3 mM EGTA (High Ncad-Fc + EGTA).

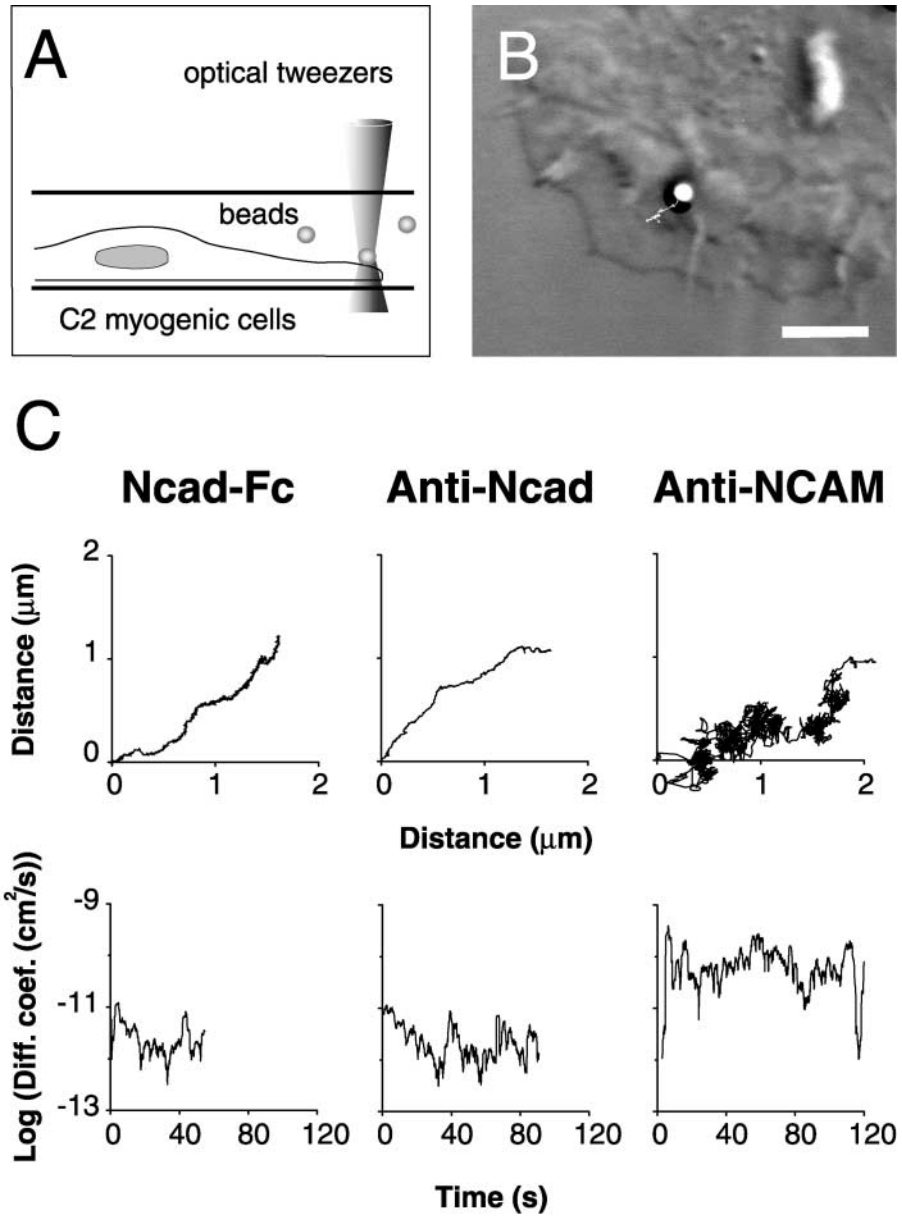

Figure 1. **Analysis by single-particle tracking of the movement of Ncad-Fc beads bound to the lamellipodia of C2 cells.** (A) Coated beads in suspension in the culture medium were trapped by the laser tweezers and held on the cell lamellipodia for 5 s to initiate bead–cell attachment. Beads that did not drift out of focus upon release of the trap were considered bound. The bead movement was followed over a period of 50–200 s and the trajectories extracted by single-particle tracking. (B) Representative trajectory of a Ncad-Fc bead superimposed on differential interference contrast image taken at the end of the recording. Bar, 5 μm. (C) Representative trajectories of Ncad-Fc, anti–N-cadherin, and anti-NCAM antibodies coated beads (X-Y plots, top) and corresponding plots of the two-dimensional diffusion coefficient as a function of time (bottom). Note the directed movement and low diffusion coefficient of the Ncad-Fc and anti–N-cadherin–coated beads. In contrast, anti–N-CAM beads remained diffusive.

efficient was very low (average, $7 \pm 11 \times 10^{-12}$ cm^2/s, $n = 15$). Moreover, the speed of Ncad-Fc beads' rearward transport (average, 0.046 ± 0.03 μm/s, $n = 15$) was similar to that of rearward-moving actin cytoskeleton reported previously (Choquet et al., 1997; Sako et al., 1998; Suter et al., 1998; Nishizaka et al., 2000), suggesting that N-cadherin molecules bound to the beads are tightly anchored to actin filaments and dragged by the actin cytoskeleton flow. Consistent with this result, the rearward transport of Ncad-Fc beads stopped at the rear of the lamellipodia where the fast actin treadmilling ends. Interestingly, N-cadherin molecules were also triggered with beads coated with polyclonal anti–N-cadherin antibodies whose movement was similar to that of Ncad-Fc beads (Fig. 1 C). Subsequently, all experiments were performed with the Ncad-Fc ligand, which has the advantage to present the homophilic adhesive properties of endogenous N-cadherin (Lambert et al., 2000). As a control, we also analyzed the movement of NCAM, an unrelated adhesion receptor known to remain unlinked to the cytoskeleton (Fig. 1 C). Anti-NCAM antibody-coated beads never adopted the oriented movement observed for Ncad-Fc beads and remained highly diffusive (diffusion coefficient, $0.8 \pm 0.5 \times 10^{-10}$ cm^2/s, $n = 11$), in agreement with previous observations (Simson et al., 1998). To directly demonstrate the implication of the actin cytoskeleton in the anchoring process and rearward transport, Ncad-Fc beads were applied at the surface of C2 cells treated by cytochalasins. Cytochalasin D at 2 μg/ml totally inhibited initial bead binding, in agreement with previous reports (Nagafuchi and Takeichi, 1988; Lambert et al., 2000). A milder actin cytoskeleton perturbation with cytochalasin B at 1 μg/ ml did not disturb the attachment of beads, but led to the inhibition of both their anchoring and rearward transport (unpublished data), directly implicating the actin cytoskeleton in these processes.

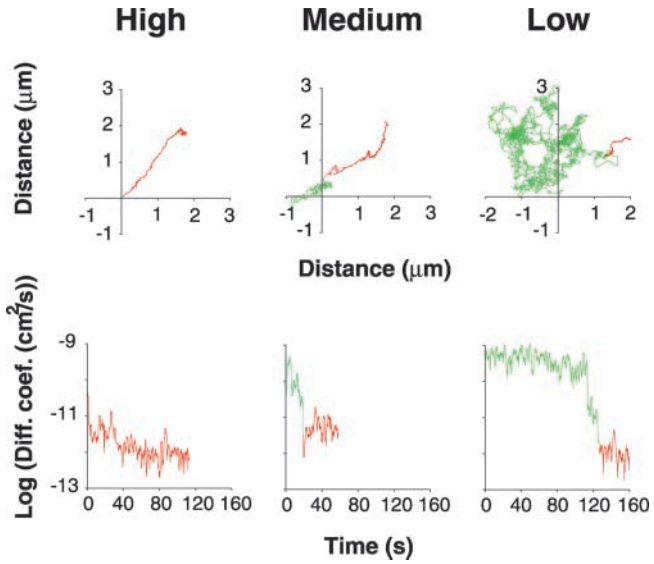

Figure 2. **Lower density Ncad-Fc beads show an initial freely diffusive phase.** Representative trajectories (X-Y plots, top) and two-dimensional diffusion coefficient versus time plots (bottom) of high, medium, and low Ncad-Fc beads. Note the biphasic behavior of the medium and low Ncad-Fc beads characterized by an initial diffusive phase (green line), followed by a sharp decrease in the diffusion coefficient and the initiation of directed movement (red line).

The movement of Ncad-Fc beads presents an initial freely diffusive phase

We postulated that the fast anchoring of Ncad-Fc or anti–N-cadherin beads may result from a massive mobilization of N-cadherin at the bead–cell contact. Hence, we hypothesized that the kinetics and/or extent of anchoring may directly depend on Ncad-Fc ligand density at the bead surface. Thus, beads were prepared with decreasing densities of Ncad-Fc corresponding to 30% (medium), 10% (low), and 1% of their maximal loading. Medium and low Ncad-Fc beads showed only a slight reduction in their cell binding capabilities (Table I). In contrast, Ncad-Fc 1% did not present binding capabilities statistically different from control Fc-coated beads (unpublished data). Despite their similar cell binding properties, medium and low Ncad-Fc beads behaved differently from high Ncad-Fc beads. Medium Ncad-Fc beads either remained diffusive or displayed a biphasic behavior characterized by an initial phase of diffusion followed by a phase of rearward transport similar to that observed with high Ncad-Fc beads. The diffusion coefficient of such beads was initially high and dropped rapidly by more than one order of magnitude when the bead adopted a directed movement (Fig. 2). The behavior of low Ncad-Fc beads was even more drastically shifted. Indeed, the majority of the low Ncad-Fc beads remained highly diffusive (diffusion coefficient, $4.6 \pm 4.4 \times 10^{-10}$ cm^2/s, $n = 25$). Nevertheless, a few low Ncad-Fc beads displayed a biphasic behavior (Fig. 2).

To confirm that such biphasic beads were initially freely diffusive and then became anchored, the mean square displacement (MSD)* was calculated and plotted as a function of time (Fig. 3). The MSD-Δt plots were then compared

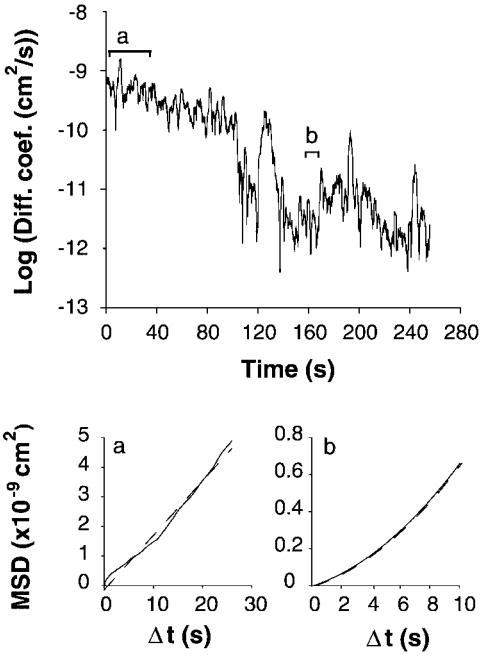

Figure 3. **Displacement analysis of biphasic low density Ncad-Fc–coated beads.** Diffusion coefficient versus time (top) and MSD of a representative biphasic medium Ncad-Fc bead were calculated as described in Materials and methods. (Bottom left) MSD was calculated within a segment of the initial phase (a), plotted as a function of time interval (plain line), and compared with theoretical MSD-Δt plots for simple Brownian diffusion (broken line). MSD increases linearly with time interval, characteristic of a simple Brownian diffusion. (Bottom right) MSD was calculated within a segment in the second phase (b), and plotted as a function of time interval (plain line). The MSD-Δt follows a parabolic curve characteristic of a unidirectional diffusion mode (broken line).

with theoretical curves for simple Brownian diffusion and directed diffusion. During the initial phase the calculated MSD-Δt plot fitted well with the theoretical simple Brownian diffusion plot. During the second phase, the MSD-Δt plot was consistent with a directed diffusion. Thus, the rapid drop in bead diffusion coefficient parallels the transition from an initial freely diffusive state to a directed transport state. Altogether, these results indicate that N-cadherin molecules bound to lower density Ncad-Fc beads are initially free to diffuse in the plasma membrane.

The kinetics of successful Ncad-Fc bead anchoring depend on the ligand density at the bead surface

Further analysis confirmed that the occurrence and kinetics of a successful anchoring of the bead were strongly dependent on the density of Ncad-Fc (Fig. 4). Indeed, in most cases (15/16) the binding of high Ncad-Fc beads induced their anchoring and rearward transport without significant latency. In contrast, only a fraction of the medium Ncad-Fc beads (5/21) were immediately anchored. The remaining beads became anchored after a significant latency or remained unanchored over the duration of the recording (120 s). Moreover, most of the low Ncad-Fc beads analyzed (11/13) remained unanchored. Thus, the kinetics of bead anchoring was directly correlated to the density of Ncad-Fc adsorbed at the bead surface, indicating that the anchoring of

*Abbreviation used in this paper: MSD, mean square displacement.

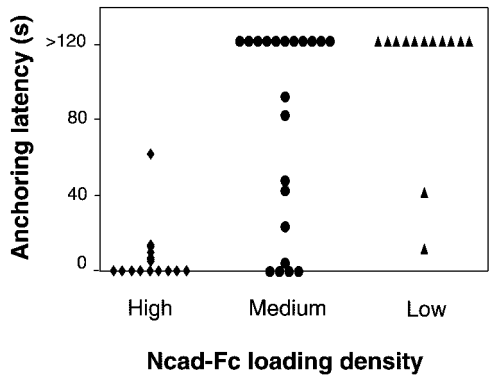

Figure 4. **Lowering the loading density of Ncad-Fc beads increases the latency to achieve anchoring.** The scattergram presents the latency of the beads to achieve anchoring as a function of the charge of the beads. Ncad-Fc beads were applied for 5 s on the cell surface as described in Fig. 1. Cell surface–bound beads were considered as anchored at the time they both display a sharp decrease in their diffusion coefficient and undergo a directed rearward movement.

N-cadherin to the cytoskeleton is an inducible process regulated by the density of N-cadherin ligand encountered at the cell surface.

To determine whether the level of Ncad-Fc bead loading density had an effect on their maximal confinement, we compared the diffusion coefficient values calculated for the differently loaded beads before and after anchoring (Table II). Interestingly, the initial diffusion coefficient of the unanchored beads was not significantly different for the three types of beads. Furthermore, the diffusion coefficients of high, medium, and low Ncad-Fc beads after anchoring were not significantly different from each other (average, 0.7 ± 1.1, 0.8 ± 0.4, and $1.0 \pm 1.7 \times 10^{-11}$ cm^2/s, respectively), indicating that the maximal confinement of anchored N-cadherin molecules was independent of ligand density.

Ncad-Fc bead anchoring is prevented by lovastatin treatment

To determine whether the strong anchoring of cadherin to the actin cytoskeleton may be regulated by intracellular factors, we wondered whether we could experimentally uncouple the initial bead binding from its subsequent anchoring. Increasing tyrosine phosphorylation has been proposed to have a negative effect on the strengthening of cadherin-mediated contacts (Ozawa and Kemler, 1998). Thus, the effect of vanadate treatment on bead behavior was evaluated (Fig. 5 A). Vanadate drastically inhibited the initial binding of Ncad-Fc beads. We previously found that the binding of Ncad-Fc beads induced local formation of filopodia and lamellipodia (Lambert et al., 2000). The small GTPases of the Rho family, regulating actin cytoskeleton dynamics and cell membrane remodeling (Hall, 1998), may be involved in these processes downstream of N-cadherin activation. In a first attempt to evaluate the role of GTPases on N-cadherin anchoring, we treated C2 cells with lovastatin (Fig. 5 A). This inhibitor of the 3-hydroxy-3-methylglutaryl coenzyme A reductase leads to a cellular depletion of farnesyl- and geranyl-geranyl-pyrophosphate, resulting in a general inhibition of GTPases likely by preventing their isoprenylation (Laufs et al., 1999). Lovastatin had very little effect on the morphology of C2 cells, which conserved their lamellipodia and did not significantly impair Ncad-Fc bead binding. However, Ncad-Fc beads bound on lovastatin-treated cells showed a dramatic inhibition of their anchoring and rearward transport, as they remained highly diffusive over the time of the experiment (Fig. 6). These results suggest that

Table II. **The confinement of anchored beads is independent of Ncad-Fc density at the bead surface**

	Diffusion coefficient (10^{-10} cm^2/s)	
Bead coverage	**Unanchored**	**Anchored**
High Ncad-Fc	1.9 ± 0.7 (5)	0.07 ± 0.11 (15)
Medium Ncad-Fc	1.3 ± 0.8 (12)	0.08 ± 0.04 (16)
Low Ncad-Fc	4.6 ± 4.4 (25)	0.10 ± 0.17 (4)

Trajectories of high-, medium-, and low-density Ncad-Fc–coated beads were analyzed, and diffusion coefficients were extracted both for the initial diffusive phase (unanchored beads) and after anchoring (anchored beads). The diffusion coefficients were calculated for each bead on successive 5-s time windows and averaged over a 15–40-s period for each phase. Values given in the table are mean values ± SDs (number of beads analyzed).

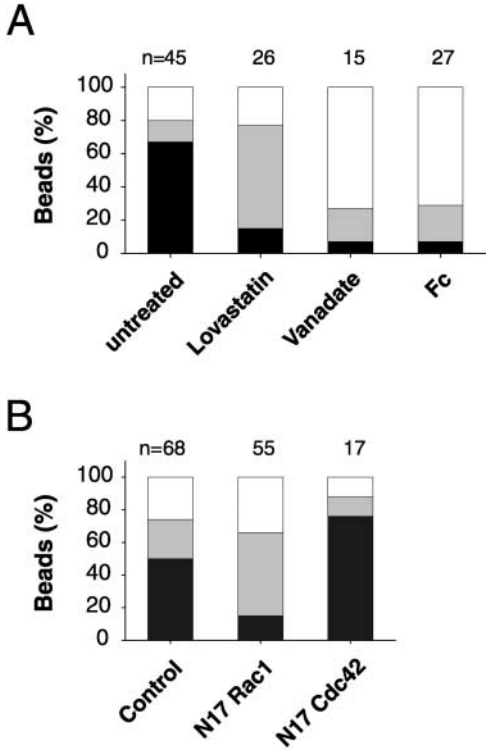

Figure 5. **Lovastatin and N17 Rac 1 inhibit Ncad-Fc bead anchoring without affecting initial binding.** (A) Cumulative histograms present the percentage of high Ncad-Fc beads anchored (black bars), bound but not anchored (gray bars), or unbound (white bars) in the 20 s after their application on lamellipodia of untreated, lovastatin-, or vanadate-treated cells. Lovastatin did not alter the bead binding capability but reduced their anchoring. Vanadate reduced Ncad-Fc bead binding to the level of binding of control Fc beads (Fc). (B) Percentage of Ncad-Fc beads anchored (black bars), bound but not anchored (gray bars), or unbound (white bars) to control, N17 Rac1–, or N17 Cdc42–expressing C2 cells. N17 Rac1 prevented bead anchoring without affecting their binding. *n* = number of beads analyzed.

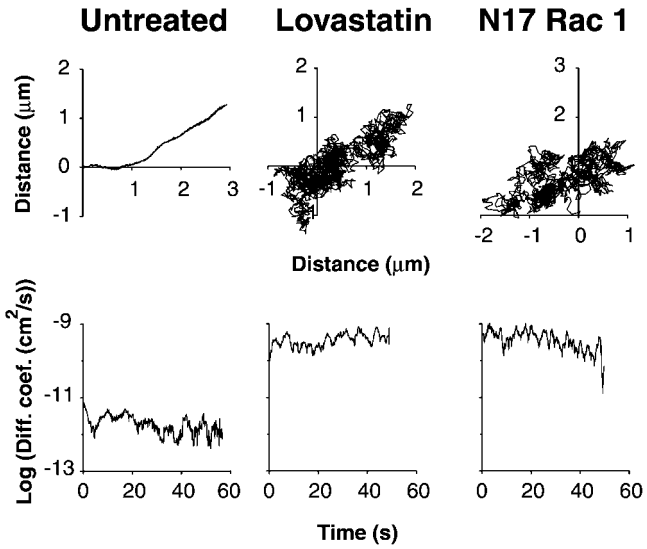

Figure 6. **Ncad-Fc beads bound at the surface of lovastatin-treated and N17 Rac1–expressing C2 cells remain highly diffusive.** Representative movement (X–Y plots, top) and diffusion coefficient versus time (bottom) of high Ncad-Fc beads bound at the surface of untreated, lovastatin-treated, and N17 Rac1–expressing C2 cells. The displacement of Ncad-Fc beads attached on lovastatin-treated or N17 Rac 1–expressing cells remained highly diffusive and nonoriented.

lovastatin impairs the tight anchoring of N-cadherin molecules to the cytoskeleton, without affecting the initial homophilic binding of N-cadherin ectodomains.

A dominant negative form of Rac1, but not of Cdc42, inhibits Ncad-Fc bead anchoring without affecting initial binding

To assess the implication of small GTPases in the anchoring step, GFP-tagged dominant negative (N17) and constitutively active (V12) forms of Rac1 and Cdc42 proteins were transfected in C2 cells, and the effect of their expression on Ncad-Fc bead binding and anchoring were analyzed. The typical morphology of the transfected cells and their actin cytoskeleton organization were similar to those previously reported (Meriane et al., 2000; Heller et al., 2001). The expression of N17 Rac1 and Cdc42 mutants did not significantly inhibit Ncad-Fc bead binding (Fig. 5 B). This absence of effect of N17 Rac1 and Cdc42 mutants was confirmed in long-term (45 min) bead–cell adhesion assays by quantifying the binding efficiency of 6-μm Ncad-Fc–coated beads on GFP-positive transfected C2 cells. Beads bound equally well on the N17 Rac1-GFP expressing cells (22 ± 3% of the cells with at least one bound bead), and the GFP-negative cells (29 ± 9%, $n = 3$). In both assays, we did not observe any effect of the V12 forms of Rac1 or Cdc42 on bead binding (unpublished data).

When the effect of Rac1 and Cdc42 mutants on Ncad-Fc bead anchoring was analyzed, we observed a drastic inhibition of the anchoring of Ncad-Fc beads bound on N17 Rac1-GFP expressing cells (Fig. 5 B). In these cells, Ncad-Fc beads remained diffusive over the time of the experiment, without directed movement (Fig. 6). By contrast, neither N17 Cdc42 (Fig. 5 B) nor the V12 forms of Rac1 or Cdc42 did alter Ncad-Fc bead anchoring (unpublished data). Thus, N17 Rac1 expression fully mimicked the lovastatin effect, inhibiting the anchoring to the cytoskeleton without affecting initial binding. These results indicate that the inhibition of Rac1, but not of Cdc42 activity, uncouples the initial homophilic binding of N-cadherin ectodomains from subsequent tight anchoring of N-cadherin to the actin cytoskeleton.

Dominant negative Rac1 or Cdc42 do not alter cell contact formation or stability

The inhibitory effect of N17 Rac1 on N-cadherin anchoring may parallel an effect on N-cadherin–mediated cell–cell contact formation or stability. Indeed, a strong inhibitory effect of N17 Rac1 and Cdc42 mutants on the formation and stability of E-cadherin mediated cell–cell contacts has been described previously in keratinocytes (Braga et al., 1997). Thus, the morphology of cell–cell contacts of C2 cells expressing transiently the N17 and V12 Rac1 mutants was analyzed after anti–β-catenin immunofluorescent staining (Fig. 7, A–B′). No major changes in the formation of cell–cell contacts nor in the accumulations of β-catenin at these sites were observed. To investigate whether perturbations of Rac1 activity may have a different effect on the recruitment of the other catenins, the cells were stained for α-catenin and p120 (Fig. 7, C–D′). Both α-catenin and p120 were accumulated similarly at cell–cell contacts in N17 Rac1-GFP–expressing cells and untransfected cells. In addition, neither N17 nor V12 forms of Cdc42 were able to prevent cell–cell contact formation and catenin accumulation in C2 cells (unpublished data). These results indicate that Rac1 and Cdc42 mutants had no major effect on cell–cell contact formation and catenin accumulation at these sites.

Dominant negative Rac1 does not alter cadherin–catenin complex recruitment and stability but impairs actin filament reorganization

To monitor the effect of N17 and V12 Rac1 mutant proteins on the bead induced recruitment of cadherin–catenin complexes, catenin immunostaining was also performed on N17 Rac1 transfected C2 cells incubated with Ncad-Fc beads for 45 min. Strong accumulations of the three catenins were detected at the contact sites between Ncad-Fc beads and GFP-positive transfected cells (illustrated for α-catenin in Fig. 8 A). No inhibitory effect of V12 Rac1, and N17 or V12 forms of Cdc42 was observed on the recruitment of α-catenin, β-catenin, and p120 at the bead–cell contact sites. The effect of Rac1 mutants on the cadherin–catenin complex stability was further evaluated by Western blotting analysis of proteins coimmunoprecipitated with β-catenin (Fig. 8 B). Equally, α-catenin was coimmunoprecipitated with β-catenin in N17 Rac1, V12 Rac1, and mock-transfected C2 cell extracts, further indicating that the α-/β-catenin interactions were not impaired when Rac1 activity was inhibited.

In parallel, we analyzed the presence in the complex of IQGAP1, as this target of Cdc42 and Rac1 has been proposed to regulate E-cadherin mediated cell adhesion by destabilizing the cadherin–catenin complex (Kuroda et al., 1998; Fukata et al., 1999). In the absence of the active forms of GTPases, IQGAP1 may interact directly with β-catenin, inducing the dissociation of α-catenin from β-catenin. In

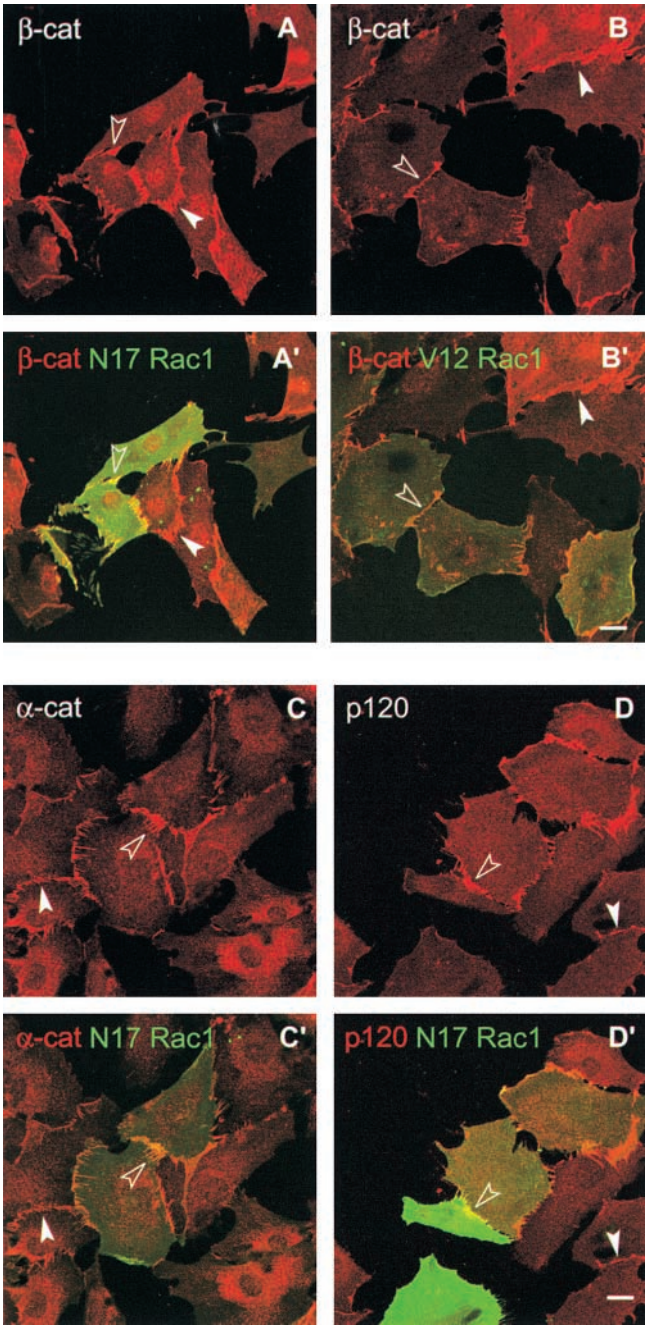

Figure 7. **Neither N17 Rac1 nor V12 Rac1 prevent the accumulation of catenins at the cell–cell contacts.** Transfected N17 Rac1-GFP (A–A′, C–C′, and D–D′) or V12 Rac1-GFP (B–B′) C2 cells were processed for immunofluorescent staining with polyclonal anti–β-catenin (A–A′ and B–B′), anti–α-catenin (C–C′) or anti-p120 (D–D′) antibodies and analyzed by confocal laser scanning microscopy. Panels show for each preparation matched three-dimensional projections of 0.5-μm confocal stacks in the red (catenins) and merge images with GFP. α-Catenin, β-catenin, and p120 were similarly accumulated at contact sites between GFP-positive cells expressing Rac1 mutants (open arrowheads) and between untransfected cells (arrowheads). Bar, 20 μm.

C2 cells, IQGAP1 was only barely detectable in β-catenin immunoprecipitates (Fig. 8 B). Furthermore, immunofluorescent staining showed that IQGAP1 was only weakly accumulated at cell–cell contacts (unpublished data), indicating

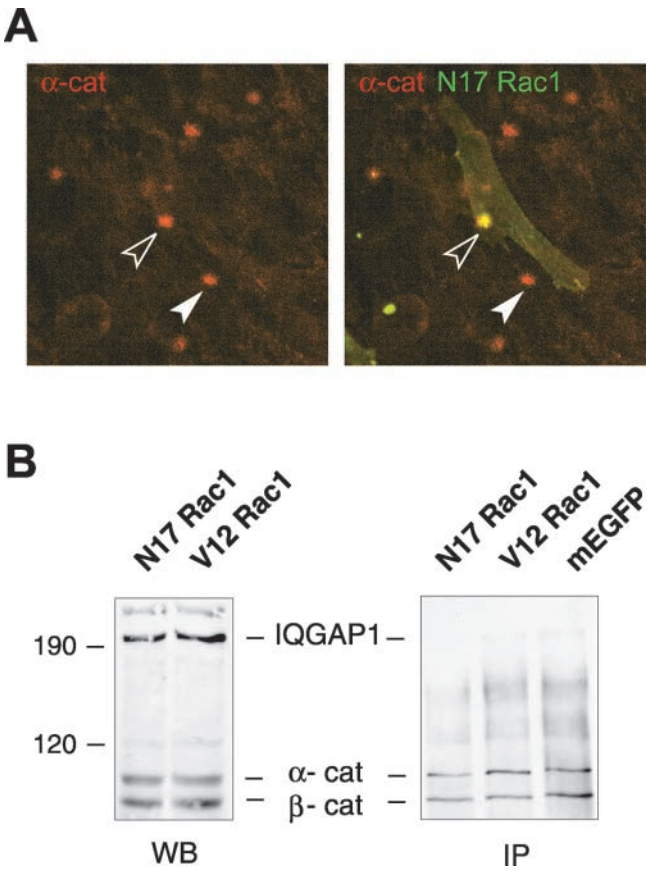

Figure 8. **N17 Rac1 does not affect the recruitment and stability of the cadherin–catenin complex.** (A) Transfected N17 Rac1-GFP C2 cells were incubated with Ncad-Fc beads for 45 min and processed for immunofluorescent staining with anti–α-catenin antibodies. The panels show matched series of three stacked 1-μm thick confocal optical sections at the level of bead–cell contact. Similar accumulations of α-catenin were detected at contact sites between Ncad-Fc beads and N17 Rac1-GFP–expressing cells (open arrowheads) and between Ncad-Fc beads and untransfected cells (arrowheads). Bar, 20 μm. (B) Puromycin-selected N17 Rac1-GFP–, V12 Rac1-GFP–, or mGFP-expressing cells were allowed to form cell–cell contacts for 5 h before proteins were extracted and analyzed by direct Western blotting with anti–β-catenin, anti–α-catenin, and anti-IQGAP1 antibodies (WB). (IP) Cadherin–catenin complexes were immunoprecipitated with anti–β-catenin antibodies and analyzed by immunoblotting with anti–β-catenin, anti–α-catenin, and anti-IQGAP1 antibodies. α-catenin coimmunoprecipitated with β-catenin at similar levels in N17 Rac1–, V12 Rac1–, and mGFP-expressing cells extracts. In contrast, IQGAP1 was barely detected in the immune complex. Molecular marker size in kD are indicated to the left.

that IQGAP1 was not a major constituent of the cadherin–catenin complex in these cells. Altogether, these observations indicate that the inhibitory effect of N17 Rac1 on N-cadherin anchoring does not result from a reduced recruitment or stability of the cadherin-catenin complexes.

The inhibitory effect of N17 Rac1 may result from a direct perturbation on actin dynamics. This hypothesis prompted us to examine the recruitment of neoformed actin filaments at the bead–cell contact. For this purpose, N17-Rac1– and V12-Rac1–expressing cells were incubated in the presence of Ncad-Fc beads and permeabilized in the presence of rhodamine-labeled actin (Fig. 9). Strong accumula-

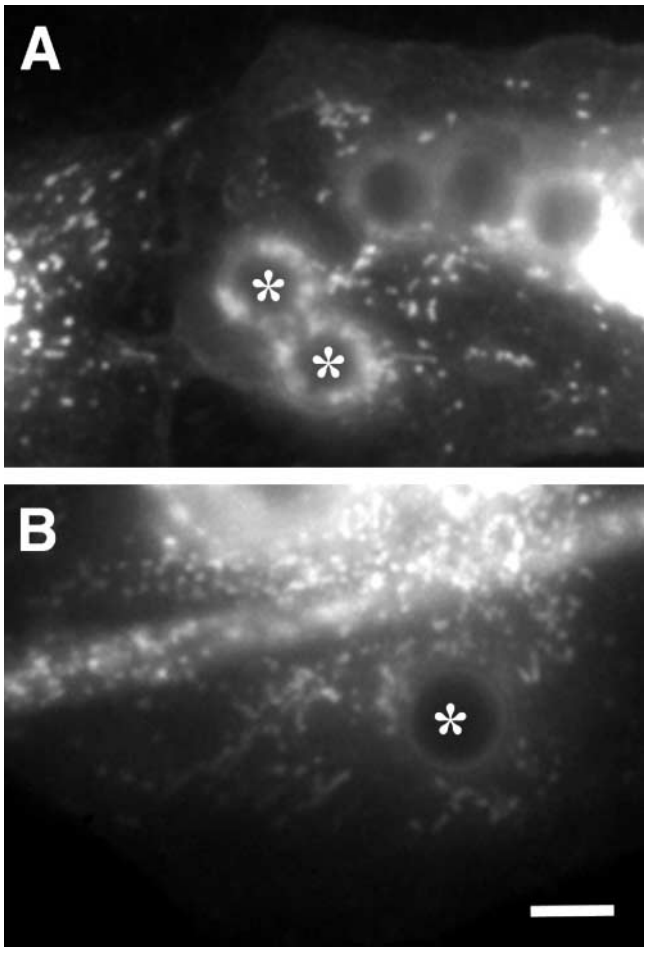

Figure 9. **N17 Rac1 interferes with actin recruitment at the Ncad-Fc bead cell contact.** V12 Rac1-GFP– (A) or N17 Rac1-GFP– (B) expressing C2 cells were incubated for 35 min in the presence of Ncad-Fc beads, and then permeabilized and incubated in the presence of rhodamine-conjugated actin for 10 min. Strong incorporation of rhodamine-labeled actin was observed at the contact sites between Ncad-Fc beads (asterisks) and V12 Rac1 expressing cells (A). These results contrast with the absence of actin incorporation at the contact sites between Ncad-Fc beads and N17 Rac1 expressing cells (B). Bar, 5 μm.

tions of rhodamine-conjugated actin were observed at the bead–cell contact in V12 Rac1 expressing cells and untransfected cells (unpublished data). In contrast, we were unable to detect these accumulations around beads in contact with N17 Rac1-transfected cells. Interestingly, rhodamine-labeled actin was strongly incorporated into focal adhesions in both conditions. These results indicate that Rac1 indeed plays an important role during actin incorporation/or recruitment at cadherin-mediated cell contacts.

Discussion

It is known that the association of the cytoplasmic domain of cadherins to actin filaments is required for cadherin ectodomain adhesive function (Nagafuchi and Takeichi, 1988). Alternatively, cadherin–cadherin adhesive interactions may regulate the anchoring of cadherin–catenin complexes to the actin cytoskeleton leading to further strengthening of cell–cell contacts and the organization of the cytoskeleton. However, our knowledge on the mechanisms underlying this mechanical anchorage remains fragmentary. We previously described an approach associating cells in culture and recombinant dimeric cadherin ectodomains immobilized on beads to activate cadherins in a controlled manner (Lambert et al., 2000). Here, taking advantage of this approach, we studied the dynamics of cadherin anchoring to the actin cytoskeleton in the very first seconds of cadherin adhesive engagement in living cells. Using video microscopy and single-particle tracking, we analyzed the movement of Ncad-Fc beads forced by optical tweezers to contact the membrane of myogenic C2 cells. To our knowledge, this work details the first report of N-cadherin movement in the plasma membrane. Our main findings are: (a) N-cadherin molecules are initially free to diffuse in the plasma membrane; (b) active N-cadherin recruitment triggered by Ncad-Fc ligand induces their strong anchoring to the actin cytoskeleton and rearward transport; (c) this anchoring is an inducible process depending on the density of homophilic ligand; (d) the activity of Rac1 is required for anchoring. These results led us to propose a model for the adhesion-triggered anchoring of cadherins to the cytoskeleton, allowing the generation of traction forces against neighboring cells.

The establishment of cell–cell contacts is initiated by the adhesive interaction of cadherin ectodomains on adjacent cells. We showed that this initial binding is regulated differentially in various cell membrane subdomains, with a preferential binding of Ncad-Fc beads on lamellipodia. The molecular bases of these differences in homophilic binding of N-cadherin molecules on the lamellipodia versus the cell body are unknown. However, lamellipodia are characterized by a highly dynamic actin cytoskeleton. Moreover, a preferential binding of fibronectin beads to lamellipodia has been reported and attributed to a better avidity of the integrin receptors for their ligand in relation to changes in their association to the actin cytoskeleton (Nishizaka et al., 2000). Thus, the adhesive properties of cadherins may be different in lamellipodia and in the cell body, in relation to actin dynamics and/or the mode of association of the cadherin cytoplasmic tail to the actin cytoskeleton.

After bead binding, we used single-particle tracking to monitor the two-dimensional movement of bead-bound N-cadherin molecules, and to determine whether their diffusion within the membrane was restricted or not. An initial diffusive phase was clearly determined for all low Ncad-Fc beads, indicating that N-cadherin molecules were initially freely diffusive in the lamellipodia. The diffusion coefficient of N-cadherin during the initial diffusive phase (3.3×10^{-10} cm^2/s) was very similar to that reported for another receptor, NCAM, known to remain unlinked to the cytoskeleton (Simson et al., 1998). It was also comparable to the diffusion coefficient determined for E-cadherin lacking the β-catenin binding site (Sako et al., 1998). Thus, our data demonstrate that N-cadherin is not tightly linked or restrained by the cytoskeleton on the free surface of lamellipodia. However, high Ncad-Fc beads were immediately diffusion restricted and pulled away from the leading edge of the cells at the speed of actin treadmilling. This diffusion restriction, inhib-

ited by actin depolymerization, can be attributed to an anchoring of N-cadherin to the actin cytoskeleton, as previously shown for β_1 integrin (Choquet et al., 1997). The behavior of these restricted N-cadherin molecules was similar to that observed by Sako et al. (1998) for an E-cadherin/α-catenin fusion mutant constitutively linked to actin filaments. Our results indicate that the homophilic binding of Ncad-Fc beads to N-cadherin triggers the transition of this receptor from a freely diffusive to a cytoskeleton anchored state with a kinetics directly dependent on the density of ligand. This process may directly mimic an adhesion-triggered anchoring of cadherin taking place during normal cell–cell contact formation.

Although this approach does not directly give insight into the molecular nature of the mechanisms involved, we propose that this anchoring may result from a ligand-induced cadherin recruitment. Indeed, Ncad-Fc beads have been shown independently to induce the recruitment of cadherin–catenin complexes by lateral diffusion in the membrane (Lambert et al., 2000). Moreover, anti–N-cadherin–coated beads became spontaneously anchored, suggesting that antibody-induced clustering by itself may induce N-cadherin anchoring. Interestingly, Sako et al. (1998) reported the existence of both anchored and freely diffusive E-cadherin molecules at the surface of transfected L cells triggered for 30 min with antibody-coated particles. Altogether, these results support a model in which cadherin molecules are free to diffuse in the cell membrane before the initiation of the adhesion process and become anchored to the actin cytoskeleton as a result of their homophilic ligand triggered recruitment. Nevertheless, we cannot exclude that the occupancy of the ectodomain by the Ncad-Fc ligand may directly activate cadherins. Alternatively, both receptor clustering and ligand occupancy may be required for cadherin activation as reported for integrins (Miyamoto et al., 1995b).

The search for intracellular factors regulating the anchoring process prompted us to test the involvement of the small GTPases Rac1 and Cdc42. The dominant negative form of Rac1 inhibited the anchoring of Ncad-Fc beads, whereas the dominant negative form of Cdc42 had no effect, indicating that N-cadherin anchoring to the cytoskeleton specifically depends on Rac1 activity. However, N17 Rac1 did not inhibit the recruitment of catenins at the bead–cell contact. Moreover, neither N17 Rac1 nor N17 Cdc42 prevented the formation of N-cadherin–mediated cell–cell contacts and the recruitment of catenins at these sites. They did not either induce the destruction of the preexistent cell contacts or the stability of the cadherin–catenin complex. Furthermore, the Rac1 and Cdc42 effector IQGAP1 did not appear significantly associated with cell–cell contacts in C2 cells, in contrast to what we and others observed in MDCK cells (Nakagawa et al., 2001; unpublished data). Braga et al. (1997) showed that N17 Rac1 or Cdc42 mutants microinjected in keratinocytes negatively regulate cadherins, although we and others did not note major effects of those mutants in transfected MDCK and C2 cells (Takaishi et al., 1997; unpublished data). These differences might be attributed to the expression level of mutant proteins achieved after microinjection or transfection. Alternatively, these differences might be related to molecular differences between cadherin species or to differences in the nature and regulation of cadherin-based cell contacts in different cell backgrounds. Indeed, very similar perturbations of GTPase activity had a differential effect on E-cadherin in keratinocytes and on VE-cadherin in endothelial cells (Braga et al., 1999). The absence of effect of N17 Rac1 on catenin recruitment observed here suggested that Rac1 may directly act on actin dynamics by regulating either actin polymerization or crosslinking. Indeed, we showed that N17 Rac1 inhibited the incorporation of rhodamine-labeled actin under the beads, arguing in favor of a role of Rac1 at the level of actin dynamics. Our results strongly specify the effect of Rac 1, as we report a specific effect of the perturbation of its activity on the functional anchoring of N-cadherin to actin, in conditions where its effect on overall cell–cell contact morphology is not detectable. This regulation by Rac1 activity may have a strong physiological relevance for the control of cell migration or contact strengthening.

Upon ligand-induced anchoring, beads were transported on the lamellipodia surface by the rearward-moving actin cytoskeleton, indicating that cadherins can mediate ligand-dependent receptor cell migration in a way similar to what has been proposed for integrins (Choquet et al., 1997). However, cadherin anchoring to the cytoskeleton shows some remarkable differences compared to integrins. The ligand-dependent anchoring of integrins triggered by the binding of fibronectin-coated beads has been shown to be reinforced upon application of a restraining force to the bead (Choquet et al., 1997). In contrast, Ncad-Fc beads spontaneously escaped the laser trap and further application of the trap over the beads was not able to restrain their movement, suggesting that cadherin-cytoskeleton anchoring was spontaneously stiff. Thus, rigidity applied on cadherin mediated contacts does not appear as a pertinent factor regulating cadherin anchoring. Conversely, prevalence and activity of N-cadherin presented by adjacent cells may be an essential parameter, in agreement with the physiological role of cadherin adhesion receptors in migration of a cell over surrounding cells. We also observed that in contrast to fibronectin-coated beads (Nishizaka et al., 2000), Ncad-Fc beads were not released at the rear of the lamellipodia. Thus, once established, the cadherin-based contacts remain stable. These results are in agreement with the fact that in many cadherin-dependent morphogenetic processes, such as border cell migration in *Drosophila* (Niewiadomska et al., 1999), convergent extension during frog gastrulation (Zhong et al., 1999), cell sorting (Friedlander et al., 1989), or neurite outgrowth (Matsunaga et al., 1988), cells maintain contact and traction with other cells during migration and rearrangement.

This ligand-dependent linkage to the cytoskeleton, and the subsequent transduction of forces across the plasma membrane, appear as an essential aspect of the functional role of cadherins in these various biological processes requiring combined cell–cell adhesion and migration. Based on the present findings, we propose a mechanistic model for cadherin action in cell rearrangement. In the case of cell sorting, the sorting between cells expressing different levels of cadherins is probably initiated by the extension of lamellipodia or filopodia contacting various distant cells. Those contacts established between higher expresser cells will be

preferentially rendered efficient to transduce mechanical forces generated by the cell's motility system, via a faster anchoring of cadherins to the actin-cytoskeleton. This ligand density kinetics advantage will favor association of these cell bodies via their efficient actin-based traction on filopodia and lamellipodia.

In conclusion, the present data show for the first time that the adhesive interactions of cadherins induce their strong anchoring to the cytoskeleton, enabling the transduction across the cell membrane of mechanical forces generated by the actin treadmilling. These findings enlighten an essential aspect of the mode of action of cadherins in developmental processes such as cell sorting, cell migration, and growth cone navigation.

Materials and methods

Preparation of Ncad-Fc–coated beads

The Ncad-Fc chimera (chicken N-cadherin ectodomain fused to the Fc fragment of the mouse IgG2b) was produced in eucaryotic cells, affinity-purified and immunoadsorbed on 1-μm latex-sulfate beads (Polyscience) as described previously (Lambert et al., 2000). Briefly, beads were washed, sonicated, and resuspended in 0.1 M borate buffer, pH 8, and incubated with goat anti–mouse Fcγ antibody (Jackson ImmunoResearch Laboratories) for 18 h at 4°C. Beads were washed with PBS, pH 7.4, blocked with PBS, 1% BSA, and charged at maximal density (high Ncad-Fc) by incubating them with a saturating quantity of Ncad-Fc in PBS/BSA for 2 h at room temperature. To obtain lower specific loading, beads were incubated with either a mixture at 30% (medium Ncad-Fc) or 10% in molecular ratio (low Ncad-Fc) of Ncad-Fc and Fc fragment (Jackson ImmunoResearch Laboratories). Beads were washed in PBS/BSA, resuspended in the same buffer, and used immediately. Beads were coated in a similar manner with either polyclonal anti–N-cadherin or anti-NCAM, by replacing the anti–mouse Fcγ antibody with an anti–rabbit Fcγ antibody (Jackson ImmunoResearch Laboratories).

Cell culture

C2 mouse myogenic cells (Yaffe and Saxel, 1977) were cultured in DME containing 10% FCS at 37°C in 7.5% CO_2. For single-particle tracking, cells were transfected 18 h before analysis, directly on coverslips by Fugen (Boehringer Mannheim) with expression vectors coding for the GFP-tagged N17 or V12 forms of Rac1 and Cdc42, a gift from Dr. Gauthier-Rouviére (CRBM/CNRS, Montpellier, France). For long-term bead cell binding assays, cells were transfected by electroporation (Easyject plus; Equibio) in OPTIMEM under 260 V, 1,500 μF. Cells were resuspended in DME containing 10% FCS and plated on 14-mm three-well glass slides at 5 10^3 cells/cm^2. For protein analysis, cells were electroporated with N17 Rac1-GFP or V12 Rac1-GFP or a membrane anchored GFP (mGFP) expression vector together with a puromycin resistance plasmid pPUR (CLONTECH Laboratories, Inc.), and then subjected to puromycin selection for 24 h (5 μg/ml). Cells were then platted at high density and replaced in puromycin free medium for another 5 h.

Video microscopy and single-particle tracking

Experiments were carried out essentially as described in Choquet et al. (1997). Briefly, C2 cells were plated at sparse density on silane-treated 22-mm glass coverslips coated with laminin, and cultured for 18 h at 37°C in a phenol red–free DME plus 10% FCS and 20 mM Hepes, pH 7.2. Cells were either untreated or treated with 50 μM pervanadate for 10 min, 100 μM lovastatin a gift from Dr. Carnac (IGM/CNRS) for 18 h, or 1 μg/ml cytochalasin B for 10 min. Cells were mounted at 37°C in medium containing coated beads (0.1–0.2% vol/vol) and visualized under differential interference contrast through a 100× Planapo objective on a C2400 Camera (Hamamatsu). An optical trap was formed with the beam of a Ti:sapphire laser (Spectra-Physics) tuned at 800 nm, 200 mW. Beads were manipulated with the optical trap, and maintained in contact with the cell surface (5–15 s) to allow their attachment. Transfected cells were identified by the green fluorescence of GFP-tagged proteins. Video images were recorded at 25 Hz on a VCR over 50–200 s for later analysis and bead positions followed using home-made software (Choquet et al., 1997) with an accuracy of 5–10 nm. For each recording, the MSD function and the apparent diffusion coefficient was calculated as previously. χ^2 or Student's *t* tests were performed on the different sets of data.

Protein extracts analysis

Cells were lysed in 50 mM Tris buffer, pH 8, 50 mM NaCl, 300 mM sucrose, 1% Triton X-100, plus protease inhibitors (Complete; Roche Diagnostics) for 20 min at 4°C. Cleared cell lysates (100 μg total proteins) were incubated first with protein A Sepharose beads (Amersham Pharmacia Biotech) loaded with rabbit nonimmune serum for 1 h at 4°C. Supernatants were then incubated for 4 h with protein A Sepharose beads loaded with a polyclonal anti–β-catenin antibody (Sigma-Aldrich). Beads were washed four times with lysis buffer. Immunoprecipitated and total protein extracts were separated on 7.5% polyacrylamide-SDS gels and immunoblotted as previously described (Lambert et al., 2000) with either polyclonal anti–β-catenin (1/5,000), anti–α-catenin (1/2,000; Sigma-Aldrich), or monoclonal anti-IQGAP1 (clone AF4, 1/2,000; Upstate Biotechnology) antibodies.

Long-term bead–cell adhesion assay and immunofluorescent staining

Long-term bead–cell binding assays were performed on cells grown for 24 h on 14-mm three-well slides as described previously (Lambert et al., 2000). Briefly, 6-μm Ncad-Fc–coated beads were incubated at a concentration of 1–2% with N17 Rac1-GFP or V12 Rac1-GFP transfected C2 cells for 45 min at 37°C. Preparations were then washed extensively with DME, 10% FCS, and fixed. The percentage of transfected and untransfected cells bearing at least one bead was determined by manual counting in three independent experiments. Alternatively, fixed cells were permeabilized and immunofluorescently stained with either polyclonal anti-p120 (1/1,000), a gift of Dr. A. Reynolds (Vanderbilt University, Nashville, TN), anti–α-catenin (1/500) or anti–β-catenin antibodies (1/500) and further analyzed with a TCS confocal microscope (Leica).

Rhodamine-conjugated actin incorporation

The experiments were performed according to Vasioukhin et al. (2000), with some modifications. Ncad-Fc beads were incubated for 35 min on C2 cells 36 h after electroporation with plasmids encoding N17 Rac1-GFP or V12 Rac1-GFP as described above. Cells were washed twice at room temperature with 20 mM Hepes, pH 7.5, 140 mM KCl, 3 mM $MgCl_2$, 2.5 mM $CaCl_2$, and then incubated for 10 min in the presence of 20 μg/ml of rhodamine-conjugated actin (Cytoskeleton), 0.02% saponin, and 1 mM ATP in the same buffer. The preparations were fixed 10 min in 0.5% glutaraldehyde and examined under a conventional fluorescence microscope (Olympus).

We thank G. Carnac for providing lovastatin and C. Gauthier-Rouvière for the various Rac1 and Cdc42 constructs. We thank also R. Schwartzman at the IFR "Biologie Intégrative," Université Paris VI and E. Etienne (Collège de France) for their help with confocal microscopy. We are grateful to A. Sobel for his continual support and members of the INSERM U440 for stimulating discussions throughout this work. We specially thank H. Enslen for his very constructive comments.

This work was supported by institutional funding from INSERM and CNRS (Programme Physique et Chimie du Vivant, PCV 1998), as well as by grants from Association Française contre les Myopathies, Association Française de Recherche contre le Cancer, La Ligue contre le Cancer, and the Conseil Régional d'Aquitaine.

Submitted: 24 July 2001
Revised: 11 March 2002
Accepted: 14 March 2002

References

Adams, C.L., and W.J. Nelson. 1998. Cytomechanics of cadherin-mediated cell-cell adhesion. *Curr. Opin. Cell Biol.* 10:527–577.

Anastasiadis, P.Z., and A.B. Reynolds. 2000. The p120 catenin family: complex roles in adhesion, signaling and cancer. *J. Cell Sci.* 113:1319–1334.

Benson, D.L., D.R. Colman, and G.W. Huntley. 2001. Molecules, maps and synapse specificity. *Nat. Rev. Neurosci.* 2:899–909.

Braga, V.M.M., L.M. Machesky, A. Hall, and N.A. Hotchin. 1997. The small GTPases Rho and Rac are required for the establishment of cadherin-dependent cell–cell contacts. *J. Cell Biol.* 137:1421–1431.

Braga, V.M.M., A. Del Maschio, L.M. Machesky, and E. Dejana. 1999. Regulation of cadherin function by Rho and Rac: modulation by junction maturation and cellular context. *Mol. Biol. Cell.* 10:9–22.

Brand-Saberi, B., A.J. Gamel, V. Krenn, T.S. Müller, J. Wilting, and B. Christ. 1996. N-cadherin is involved in myoblast migration and muscle differentia-

tion in the avian limb bud. *Dev. Biol.* 178:160–173.

Choquet, D., D.P. Felsenfeld, and M.P. Sheetz. 1997. Extracellular matrix rigidity causes strengthening of integrin-cytoskeleton linkages. *Cell.* 88:39–48.

Felsenfeld, D.P., P.L. Schwartzberg, A. Venegas, R. Tse, and M.P. Sheetz. 1999. Selective regulation of integrin-cytoskeleton interactions by the tyrosine kinase Src. *Nat. Cell Biol.* 1:200–206.

Friedlander, D.R., R.M. Mège, B.A. Cunningham, and G.M. Edelman. 1989. Cell sorting-out is modulated by both the specificity and amount of different cell adhesion molecules (CAMs) expressed on cell surfaces. *Proc. Natl. Acad. Sci. USA.* 86:7043–7047.

Fukata, M., S. Kuroda, M. Nakagawa, A. Kawajiri, N. Itoh, I. Shoji, Y. Matsuura, S. Yonehara, H. Fujisawa, A. Kikuchi, and K. Kaibuchi. 1999. Cdc42 and Rac1 regulate the interaction of IQGAP1 with β-catenin. *J. Biol. Chem.* 274:26044–26050.

Goichberg, P., and B. Geiger. 1998. Direct involvement of N-cadherin-mediated signaling in muscle differentiation. *Mol. Biol. Cell.* 9:3119–3131.

Hall, A. 1998. Rho GTPases and the actin cytoskeleton. *Science.* 279:509–514.

Hatta, K., A. Nose, A. Nagafuchi, and M. Takeichi. 1988. Cloning and expression of cDNA encoding a neural calcium-dependent cell adhesion molecule: its identity in the cadherin gene family. *J. Cell Biol.* 106:873–881.

Heller, H., E. Gredinger, and E. Bengal. 2001. Rac 1 inhibits myogenic differentiation by preventing the complete withdrawal of myoblasts from the cell cycle. *J. Biol. Chem.* 276:37307–37316.

Kemler, R. 1993. From cadherins to catenins: cytoplasmic protein interactions and regulation of cell adhesion. *T.I.G.* 9:317–321.

Kuroda, S., M. Fukata, M. Nakagawa, K. Fujii, T. Nakamura, T. Ookubo, I. Izawa, T. Nagase, N. Nomura, H. Tani, et al. 1998. Role of IQGAP1, a target of the small GTPases Cdc42 and Rac1, in regulation of E-cadherin-mediated cell-cell adhesion. *Science.* 281:832–835.

Kusumi, A., Y. Sako, and M. Yamamoto. 1993. Confined lateral diffusion of membrane receptors as studied by single particle tracking (nanovid microscopy). Effects of calcium-induced differentiation in cultured epithelial cells. *Biophys. J.* 65:2021–2040.

Kusumi, A., K. Suzuki, and K. Koyasako. 1999. Mobility and cytoskeletal interactions of cell adhesion receptors. *Curr. Opin. Cell Biol.* 11:582–590.

Lambert, M., F. Padilla, and R.M. Mège. 2000. Immobilized dimers of N-cadherin-Fc chimera mimic cadherin-mediated cell contact formation: contribution of both inside-out and outside-in signals. *J. Cell Sci.* 113:2207–2219.

Lauffenburger, D.A., and A.F. Horwitz. 1996. Cell migration: a physiological integrated molecular process. *Cell.* 84:359–369.

Laufs, U., D. Marra, K. Node, and J.K. Liao. 1999. 3-hydroxy-3-methylglutaryl-CoA reductase inhibitors attenuate vascular muscle proliferation by preventing Rho GTPase-induced down-regulation of p27(Kip1). *J. Biol. Chem.* 274:21926–21931.

Matsunaga, M., K. Hatta, A. Nagafuchi, and M. Takeichi. 1988. Guidance of optic nerve fibres by N-cadherin adhesion molecules. *Nature.* 334:62–64.

Mège, R.M., D. Goudou, C. Diaz, M. Nicolet, L. Garcia, G. Géraud, and F. Rieger. 1992. N-cadherin and N-CAM in myoblast fusion: compared localisation and effect of blockade by peptides and antibodies. *J. Cell Sci.* 103: 897–906.

Meriane, M., P. Roux, M. Primig, P. Fort, and C. Gauthier-Rouvière. 2000. Critical activities of Rac1 and cdc42Hs in skeletal myogenesis: antagonistic effects of JNK and p38 pathways. *Mol. Biol. Cell.* 11:2513–2528.

Miyamoto, S., S.K. Akiyama, and K.M. Yamada. 1995a. Synergistic roles for receptor occupancy and aggregation in integrin transmembrane function. *Science.* 267:883–885.

Miyamoto, S., H. Teramoto, O.A. Coso, J.S. Gutkind, P.D. Burbelo, S.K. Akiyama, and K.M. Yamada. 1995b. Integrin function: molecular hierarchies of cytoskeletal and signaling molecules. *J. Cell Biol.* 131:791–805.

Nagafuchi, A., and M. Takeichi. 1988. Cell binding function of E-cadherin is regulated by the cytoplasmic domain. *EMBO J.* 7:3679–3684.

Nakagawa, M., M. Fukata, M. Yamaga, N. Itoh, and K. Kaibuchi. 2001. Recruitment and activation of Rac 1 by the formation of E-cadherin-mediated cell-cell adhesion sites. *J. Cell Sci.* 114:1829–1838.

Niewiadomska, P., D. Godt, and U. Tepass. 1999. DE-cadherin is required for intercellular motility during *Drosophila* oogenesis. *J. Cell Biol.* 144:533–547.

Nishizaka, T., Q. Shi, and M.P. Sheetz. 2000. Position-dependent linkages of fibronectin-integrin-cytoskeleton. *Proc. Natl. Acad. Sci. USA.* 97:692–697.

Ozawa, M., and R. Kemler. 1998. Altered cell adhesion activity by pervanadate due to the dissociation of α-catenin from the E-cadherin catenin complex. *J. Biol. Chem.* 273:6166–6170.

Pertz, O., D. Bozic, A.W. Koch, C. Fauser, A. Brancaccio, and J. Engel. 1999. A new crystal structure, Ca^{2+} dependence and mutational analysis reveal molecular details of E-cadherin homoassociation. *EMBO J.* 18:1738–1747.

Radice, G.L., H. Rayburn, H. Matsunami, K.A. Knudsen, M. Takeichi, and R.O. Hynes. 1997. Developmental defects in mouse embryos lacking N-cadherin. *Dev. Biol.* 181:64–78.

Sako, Y., A. Nagafuchi, S. Tsukita, M. Takeichi, and A. Kusumi. 1998. Cytoplasmic regulation of the movement of E-cadherin on the free cell surface as studied by optical tweezers and single particle tracking: corralling and tethering by the membrane skeleton. *J. Cell Biol.* 140:1227–1240.

Shapiro, L., A.M. Fannon, P.D. Kwong, A. Thompson, M.S. Lehmann, G. Grübel, J.-F. Legrand, J. Als-Nielsen, D.R. Colman, and W.A. Hendrickson. 1995. Structural basis of cell-cell adhesion by cadherins. *Nature.* 374:327–337.

Simson, R., E.D. Sheets, and K.A. Jacobson. 1995. Detection of temporary lateral confinement of membrane proteins using single-particle tracking analysis. *Biophys. J.* 69:989–993.

Simson, R., B. Yang, S.E. Moore, P. Doherty, F.S. Walsh, and K.A. Jacobson. 1998. Structural mosaicism on the submicron scale in the plasma membrane. *Biophys. J.* 74:297–308.

Sterba, R.E., and M.P. Sheetz. 1998. Basic laser tweezers. *Methods Cell Biol.* 55:29–41.

Suter, D.M., L.D. Errante, V. Belotserkovsky, and P. Forscher. 1998. The Ig superfamily cell adhesion molecule apCAM, mediates growth cone steering by substrate-cytoskeletal coupling. *J. Cell Biol.* 141:227–240.

Takaishi, K., T. Sasaki, H. Kotani, H. Nishioka, and Y. Takai. 1997. Regulation of cell–cell adhesion by Rac and Rho small G proteins in MDCK cells. *J. Cell Biol.* 139:1047–1059.

Takeichi, M. 1988. The cadherins: cell-cell adhesion molecules controlling animal morphogenesis. *Development.* 102:639–655.

Vasioukhin, V., C. Bauer, M. Yin, and E. Fuchs. 2000. Directed actin polymerization is the driving force for epithelial cell-cell adhesion. *Cell.* 100:209–219.

Yaffe, D., and O. Saxel. 1977. Serial passaging and differentiation of myogenic cells isolated from dystrophic mouse muscle. *Nature.* 270:725–727.

Yap, A.S., W.M. Brieher, and B.M. Gumbiner. 1997. Molecular and functional analysis of cadherin-based adherens junctions. *Annu. Rev. Cell Dev. Biol.* 13: 119–146.

Zhong, Y., W.M. Brieher, and B.M. Gumbiner. 1999. Analysis of C-cadherin regulation during tissue morphogenesis with an activating antibody. *J. Cell Biol.* 144:351–359.